44 MW

LA-UR-00-3183

Approved for public release; distribution is unlimited.

Title: LIGA FOR LOBSTER?

Author(s): Andrew G. Peele, Thomas H. K. Irving, Keith A. Nugent:
School of Physics, University of Melbourne, Australia.
Derrick C. Mancini, Mike Moldovan: Argonne National Laboratory
Todd R. Christenson:Sandia National Laboratory
Rob Petre: Laboratory for High Energy Astrophysics,
NASA Goddard Space Flight Center
Steven P. Brumby: LANL NIS-2

Submitted to: SPIE International Symposium on Optical Science and Technology
San Diego, California, 30 July-4 August 2000

Los Alamos
NATIONAL LABORATORY

DISCLAIMER

DISCLAIMER

Portions of this document may be illegible in electronic image products. Images are produced from the best available original document.

LIGA for Lobster?

Andrew G. Peele*[a], Thomas H. K. Irving[a], Keith A. Nugent[a], Derrick C. Mancini[b], Mike Moldovan[b], Todd R. Christenson[c], Rob Petre[d], Steven P. Brumby[e]

[a]School of Physics, University of Melbourne, Parkville 3010, Australia

[b]Argonne National Laboratory, 9700 S. Cass Avenue, Argonne, IL 60439

[c]Sandia National Laboratory, Albuquerque, NM, USA

[d]Laboratory for High Energy Astrophysics, Goddard Space Flight Center, NASA, Greenbelt, MD 30771 USA

[e]Space and Remote Sensing Sciences, Los Alamos National Laboratory, Los Alamos, New Mexico 87545, USA.

ABSTRACT

The prospect of making a lobster-eye telescope is drawing closer with recent developments in the manufacture of microchannel-plate optics. This would lead to an x-ray all-sky monitor with vastly improved sensitivity and resolution over existing and other planned instruments. We consider a new approach, using deep etch x-ray lithography, to making a lobster-eye lens that offers certain advantages even over microchannel-plate technology.

Keywords: lobster-eye optics, x-ray optics, LIGA, lithography

1. INTRODUCTION

The lobster-eye optic for x-ray astronomy purposes was first proposed in 1979[1]. The device consists of an array of square channels arranged so that the long axis of each channel is radial to the center of a sphere. Grazing incidence x-rays can undergo a single reflection to form a focal arm (Figure 1). Reflections from two orthogonal walls within a channel can reflect into a central focus area (Figure 2). When the channel length to diameter is optimized approximately 33%[2] of the incident flux may be reflected into the central focus, which, in an ideal system, has a size equal to the channel diameter. The actual efficiency is modified by the reflectivity of the walls and by any imperfections in the array. At the time of the first proposal, the technology to build an operable x-ray lobster-eye optic did not exist. Since then developments in the opto-electronics industry have produced square-pore microchannel plates (MCPs) that are of extremely high quality and a correspondingly high quality cruciform focal image has been obtained[3] (Figure 3). An extensive study into the feasibility of an x-ray all-sky monitor using MCP technology concluded that such a device would reach unprecedented levels of sensitivity and resolution[4]. Current MCPs are nearing the baseline parameters required to make a telescope that will perform at this level[3,5]. However, there exist areas for improvement that could enhance telescope performance even further. In particular,

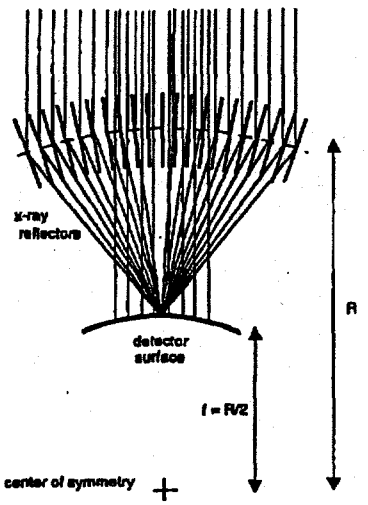

Figure 1: Cross section of a lobster-eye optic. Rays undergoing reflection from channel walls will be reflected into a focal line or 'arm'.

*Correspondence: Email: peele@optics.ph.unimelb.edu.au; Telephone: 613 8344 5458; Fax: 613 9347 4783

the theoretical telescope resolution of less than 0.1 arc-second is significantly smaller than the best demonstrated resolution of order 1 arc-minute. Current MCPs are made of glass, which has relatively low x-ray reflectivity at the designed telescope bandpass (~ 0.5 – 3.5 keV). There are indications that coating may be possible[6,7], although it is not yet clear that the coating will be of sufficient quality to improve performance. A technology that produced the lobster-eye optic in a metal such as Nickel would offer an improvement in reflectivity over the glass MCPs. Finally, MCPs are made in a relatively small format (up to ~ 4 cm x 4 cm). Current designs feature modules of ~ 40 cm x 40 cm which require tiling with many MCPs. A technology that produced the lobster-eye optic in a larger format would require less tiling and so reduce potential for misalignment errors.

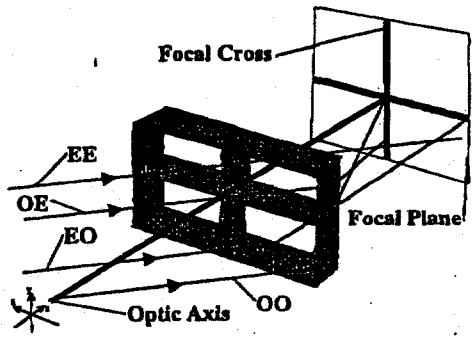

Figure 2: Reflections from different channel walls are redirected to form different parts of the cruciform focal pattern.

We have previously investigated an electro-chemical method of etching Silicon as a way of making a lobster-eye array and determined some of the parameters that must be met in order for high-quality focusing[8]. In this paper we investigate whether a lithography process, known as LIGA, has the potential to improve on the existing MCP technology. We choose LIGA as it has the potential to provide all the improvements listed above.

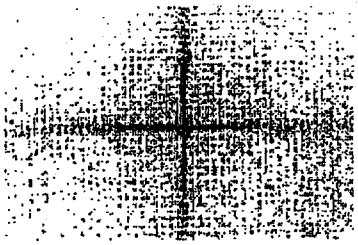

Figure 3: Example of high quality x-ray image produced by a flat MCP using a point source at 1.5 keV.

2. LIGA

LIGA is a German acronym based on the words *lithographie*, *galvanoformung*, and *abformung*. LIGA is a micro-machining technique (see Figure 4 for a schematic) that involves exposing a substrate (typically poly-methyl-methacrylate (PMMA)) through a mask to an intense beam of parallel x-rays (only available from a synchrotron). Once exposed the PMMA is developed so as to dissolve away the exposed portion. The remaining PMMA structure is then electroplated to create the desired structure in metal. The composite metal and PMMA structure is then re-exposed and the remaining PMMA is removed as before. Finally, the metal structure may be separated from the substrate metal layer by dissolving a thin intermediate sacrificial metal layer. For a high-energy exposure suitable for etching deep structures the mask itself may be a "daughter" mask that has also been made by LIGA. Initially exposure through an optical mask and development of a photoresist is used to make a conventional photolithographic mask. Exposing PMMA to soft x-rays through the photomask, then developing and electroplating the resulting structure, as above, makes the daughter mask. Typically, a daughter mask will be made of a high-Z material, such as gold, in order to provide the maximum contrast during the high-energy exposure.

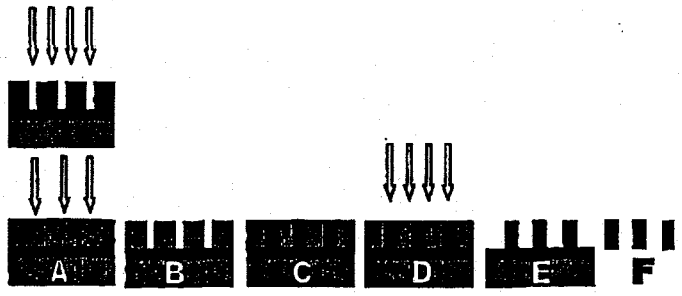

Figure 4: Schematic of steps in LIGA. A. Expose through mask onto substrate. B. Develop substrate down to metal layer to remove exposed portion. C. Electroplate. D. Re-expose. E. Develop to remove remaining substrate. F. Separate structure from sacrificial metal layer.

We require a high-energy exposure to make a lobster-eye optic as the optimal channel depth can be more than 30 times the width of an individual channel. For 30 μm channels the depth of the exposure is therefore of the order of 1 mm. Such tall structures standing on such a narrow base can lead to adhesion problems in the intermediate PMMA structure (step B in Figure 4) whereby the tall columns of PMMA can loose contact with the metal layer and move or fall over. In this "proof of concept" investigation we

initially avoid this issue by investigating a lower aspect ratio structure made using a lower energy exposure.

3. Results

We produced a set of ~10 x 13 mm Nickel test samples with various width channels, all 200 μm deep. The exposure was made at the CAMD facility operated by Louisiana State University. We describe here the results for a sample with 30 μm channels, as the ~7:1 aspect ratio was the most likely to produce an observable lobster-eye focus. In terms of the geometry and surface parameters we measured, the sample discussed was typical of the remainder in the set.

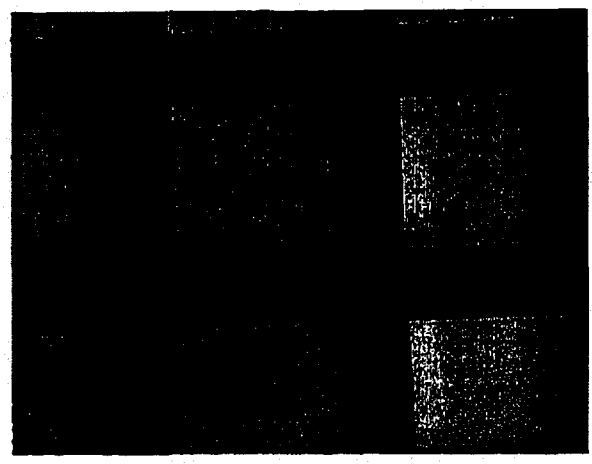

Figure 5: LIGA test sample. Channels are 30 μm wide.

3.1 Geometry

Figure 5 shows a microscope image of the test structure. It can be seen that the squareness and alignment of the channel openings is at least as good as for an MCP (Figure 6). We have taken a careful sequence of microscope images and using an automated routine that locates channel corners[9] we have measured certain of the array parameters. Importantly, we see that channel rotations (0.13 mrad standard deviation) are improved over the case for MCPs (20 mrad standard deviation). We have also measured the channel opening at the front and the back face of the array to determine the amount of channel taper. We find that taper is 13% over 200 μm. For our 30 μm channels this corresponds to a taper half-angle of 8.6 mrad (0.5°). This amount of channel deviation from the ideal case is significantly more than the 0.2 mrad channel tilts found in a high-quality system[8] and will affect the focus.

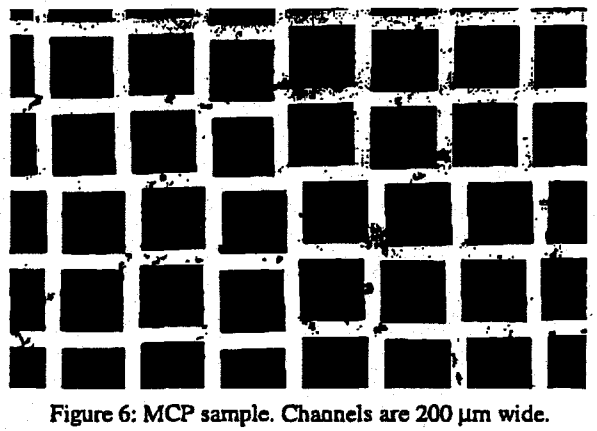

Figure 6: MCP sample. Channels are 200 μm wide.

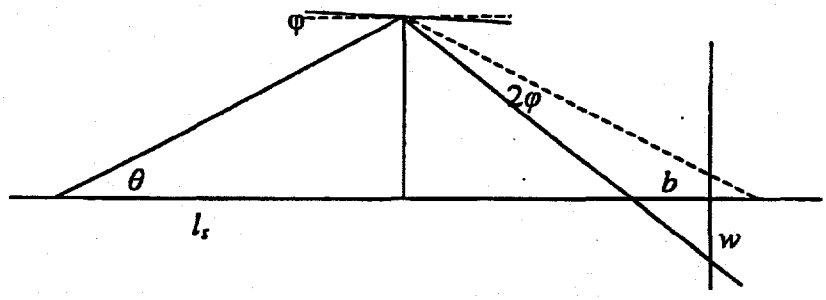

Figure 7: Schematic for calculating focal shift (w) and defocus (b) for tapered channel with taper angle 2φ for a source distance l_s and a ray leaving the source at an angle θ.

As each reflecting surface is tilted, rays are deflected by twice the tilt, or, in our case, twice the taper half-angle from the direction they would reflect in the ideal case. Rays reflecting from the upper walls of channels are deflected downwards, while rays reflecting from the lower walls are deflected upwards, thus splitting the focal arm. From Figure 7 we can calculate the deflection (w) as follows:

$$b = l_s\left(1 - \frac{\tan\theta}{\tan(\theta + 2\phi)}\right), \qquad [1]$$

$$w = b\tan(\theta + 2\phi), \qquad [2]$$

where the symbols are defined in Figure 7. For our experimental arrangement (described below) we have θ = [-0.015,0.015] radians, l_s = 0.43 m, and φ = 0.0086 radians. Accordingly, we expect a deflection from the straight through direction of ~7.4 mm. Thus we expect a focal pattern of two parallel focal arms separated by ~15 mm, with two orthogonal arms with the same separation. At the intersections of the arms there is additional flux corresponding to approximately one-quarter of the expected central focus flux. The effect is shown in the modeling section below.

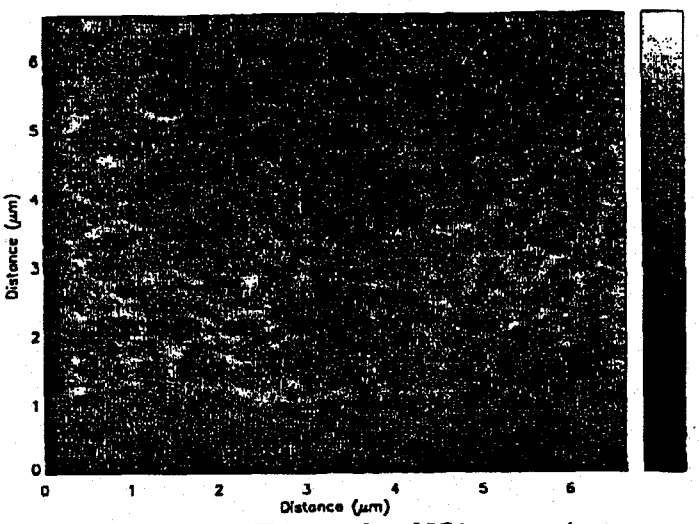

Figure 8: AFM scan of our LIGA test sample.

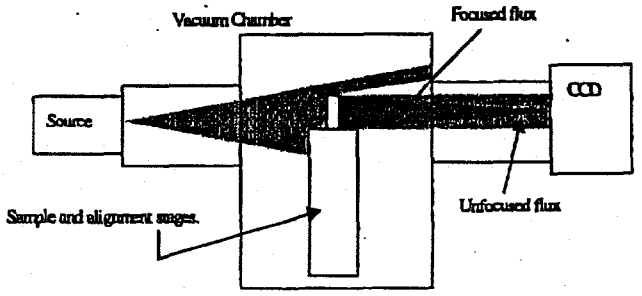

Figure 9: Experimental arrangement. The incident flux is defined by a pinhole close to the source.

3.2 Surface Quality

The problem of how to measure surface roughness on the inside of channels walls is a difficult one. Conventional AFM cantilevers are too large to fit into much of our holes and breaking or cutting open the sample introduces stresses and debris that affect the measured values. Accordingly, we incorporated a border of ~200 μm holes around our test sample that were open to AFM measurement. While the surrounding geometry of these surfaces is different than the channels we are interested in, all the exposure, development and plating conditions are necessarily identical and we assume that similar micro-roughness features result. We measured micro-roughness in areas of ~ 6 μm x 6 μm and obtained root mean square values between 10 nm and 30 nm. It can be seen from Figure 8 that the surface has a cratered appearance consistent with the development process.

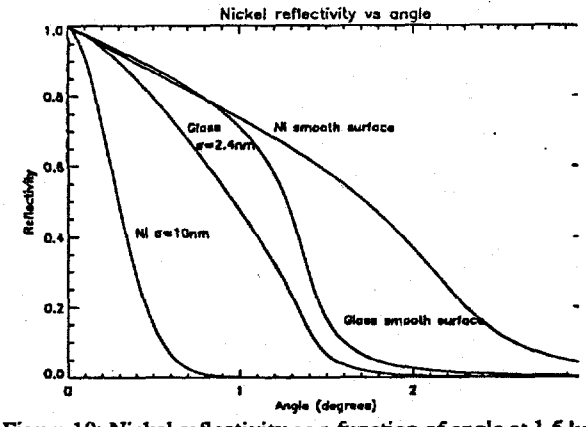

Figure 10: Nickel reflectivity as a function of angle at 1.5 keV, showing reflectivity for a perfectly smooth surface and a surface with 10 nm root mean square roughness. Also shown is the reflectivity for a common MCP glass composition for a smooth surface and a surface with 2.4 nm root mean square roughness (again a typical MCP figure).

3.3 X-ray tests

The acid test of whether a test sample will function as an x-ray lobster-eye optic is to perform an x-ray focusing test. We used the soft x-ray test facility at the University of Melbourne. The facility uses a standard laboratory x-ray source with a choice of Aluminum or Magnesium target. The x-ray beam path is evacuated and a variable aperture located close to the source defines the beam, we used an aperture diameter of ~ 500 μm for these tests. Remotely operated stages allow alignment of the sample within the evacuated chamber, which is at a distance of 430 mm from the aperture. The detector, also at a distance of 430 mm from the sample, is a bare back-thinned, charge-coupled device (CCD) manufactured by Scientific Imaging Technologies Inc.[10] Figure 9 shows the experimental arrangement. The AFM measurements suggest that reflectivity will be extremely low (see Figure 10) so we might expect that the formation of the focal arms would be suppressed. It is possible to improve the likelihood of observing reflections by

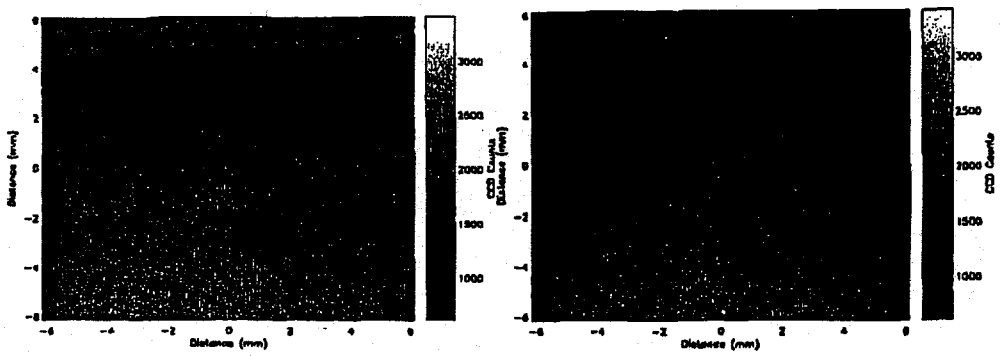

Figure 11: X-ray CCD images showing horizontal focal arm. Flux passing above the array and through a border of rectangular guidance holes about the edge of the array can be seen at the top of the images. Flux passing straight through channels towards the center of the array without reflecting can be seen at the bottom of the images. In the right hand image, the array has been rotated about the horizontal axis thus shifting the horizontal focal arm upwards.

rotating the array about either the *x*- or *y*- axis so that the more of the length of a channel intercepts the incident beam. Using this alignment we have been able to observe one of the focal arms from the cruciform lobster-eye focal structure (Figure 11). For this image the taper is towards the source. We also reversed the sample, so that the taper was towards the detector, and attempted to observe the split focal arms simultaneously, but without success. As described in the modeling section (below), this is expected. Figure 12 shows a difference plot for the two images in Figure 11 that has been summed over the rows to highlight the vertical structure in the image. The focal arm from the first image and the shifted arm from the rotated second image stand out clearly. It can also be seen that flux at the bottom of the image is greater in the first image than the second image and vice versa for flux at the top of the image. This is because rotating the array has brought channels at the top into line with the incident beam allowing more flux through while channels at the bottom present less open area.

The presence of any focusing is more than was expected from this initial test sample and indicates that the surface quality is, on average, better than expected. This represents the first indication of x-ray lobster-eye focusing from a LIGA-produced sample. It also represents the first indication of x-ray lobster-eye focusing from an integrated structure other than an MCP (although there have been examples of optics constructed by assembling individual pieces such as individual square capillaries[11] or by making arrays from flat reflectors arranged in two crossed cylindrical arrays to approximate a lobster-eye arrangement[12]). The focal arm we do image is also considerably broader than expected for a high quality image (Figure 3). This is due in part to the fact that a relatively large source pinhole was used (~ 0.5 mm), also diffuse scattering from the rough surface will broaden the expected focal distribution as will the presence of random tilts along the channels. To estimate the relative importance of some of these effects we turn to our simulation model.

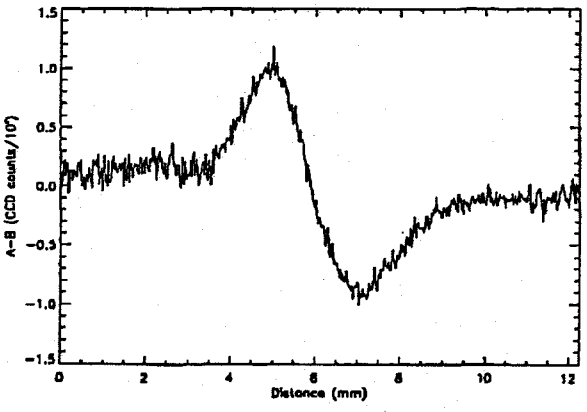

Figure 12: Difference plot for the images in Figure 11. The difference between the two images is taken and the rows summed to give a one-dimensional plot. The focal arm from the first image is the peak and the focal arm from the second image appears as the inverted peak.

4. Modeling

We use a ray trace simulation that uses a minimum of free parameters. Previous models have all left parameters such as channel location, rotation, and squareness free to be fit within the simulation[3,13,14]. With our new algorithm[9] these parameters are all incorporated directly from the input locations of the channel corners. We used the corner locations at the front of the array and defined the channel walls by projecting those corners to the back face of the array with some random tilt and the measured average taper. With the array defined in this way the only important remaining free parameters involve

reflections from the surface of the array. We incorporate a simple scattering model based on perturbing the specular direction of the reflected ray with an even distribution in a cone about the specular direction. The likelihood of a reflection taking place is modified by the Debye-Waller factor[15] so that:

$$R_{rough} = R_{smooth} \exp\left[-\frac{1}{2}\left(\frac{4\pi\sigma \sin\theta}{\lambda}\right)^2\right] \qquad [3]$$

where σ is the root mean square surface roughness, θ is the grazing angle of incidence, λ is the wavelength of the radiation and R_{rough} and R_{smooth} are the roughness-modified and smooth surface reflectivities respectively.

Figure 13 shows our modeling of the experimental result shown in Figure 11. The model includes an approximation to the non-uniform source distribution and the source spectrum. We are able to qualitatively reproduce the experimental data using random channel tilts that obey a normal distribution with a standard deviation of 0.7 mrad, surface roughness of 10 nm and scattering into a cone angle of 0.5 mrad. The source size and distance and detector features are all as used in the x-ray tests described above. The array is rotated by 14 mrad about the optic axis so that the position of the focal arm matches that in the data. The taper of the channels in the simulation is towards the source, although a similar image can be obtained with the appropriate array rotation when the taper direction reversed. This is because the single focal arm seen is produced by reflections from either the upper or lower wall only of the array channels. The fit roughness of 10 nm is also in agreement with the lower end of our AFM measurement of 10 - 30 nm, particularly when we consider the simplistic approach taken. For a fuller treatment we would have to consider the surface statistics in the range of spatial frequencies sampled by the x-ray flux, which would be different in turn to the range sampled by an AFM measurement.

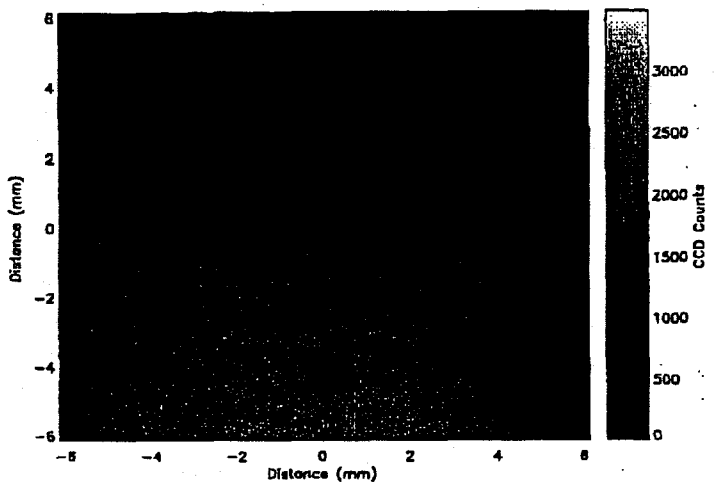

Figure 13: Simulation model results for the experimental result shown in Figure 11.

Figure 14 shows modeled images where we have reversed the direction of the taper and removed the array rotation about the y-axis. The area of the detector has also been increased so that all features of

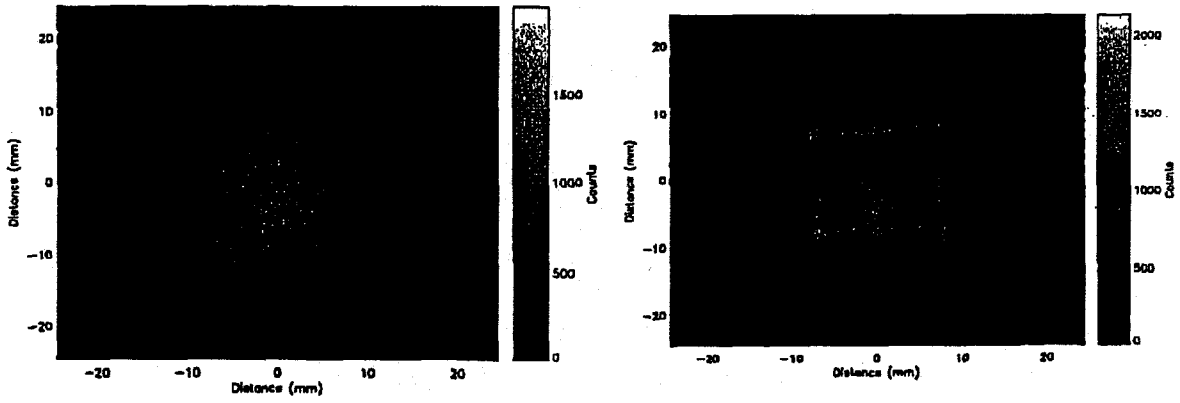

Figure 14: Simulations for our test sample. On the left, the same parameters as for Figure 13 have been used but with no array rotation about the y-axis and the taper is towards the detector. On the right we have used perfect reflectivity and no scatter. The non-uniform source distribution can be seen in both images. On the right it can also be seen that the source illumination was not aligned with the optic axis, which passes through the center of the array. The rotation of the sample in the plane of the image is to match the experimental position. Note also the change in scale, which is to allow the full array to be seen.

the array can be seen. The left-hand image shows the image for our experimental parameters and the right-hand image shows the same arrangement but with zero roughness and scatter. In this aligned position only a small section of each channel wall is available for reflection and most of the incident flux passes straight through the array. Consequently, it is not possible to observe the split focal arm pattern. Rotating the array about the *y*-axis helps improve the efficiency for either the upper or lower walls of all channels (similarly with left and right walls for an *x*-axis rotation), but this decreases the efficiency for the opposite wall. When the rotation is large enough (as in our case) the opposite wall is shadowed and no reflections are possible. The right hand image shows where the focal arms would appear if reflectivity were perfect. The separation is ~ 15 mm as expected from our earlier calculation.

5. Future Work

For a functioning lobster-eye telescope we must increase the aspect ratio from the ~ 7:1 in our test sample to ~ 50:1. Aspect ratio may be reached by moving to deep-etch LIGA techniques (requiring the use of a secondary or daughter mask) or by stacking of lower aspect ratio structures such as our test sample. The former method is to be preferred as another development required is curvature and it is easier to envisage methods of curving a single piece (for instance by heat slumping on a mandrel as is done for MCPs) than it is for multiple stacked pieces. We have begun preliminary deep-etch LIGA work and have already demonstrated the production of the intermediate step of high aspect ratio columns in PMMA. In Figure 15 a section of broken column (~ 800 μm long and ~20 μm wide) from a section of the mask where we were attempting a high aspect ratio can be seen lying on top of columns that are ~80 μm wide. It can be seen that there is no sign of tapering in the high aspect column and that the regularity of the wider columns is extremely good. It can be seen that a column in the top right of Figure 15 has become detached from the base and has moved. This "adhesion" problem is currently the limiting factor in pushing to very high aspect ratios and we are currently investigating ways of promoting the attachment of the PMMA columns to the metal layer once etched.

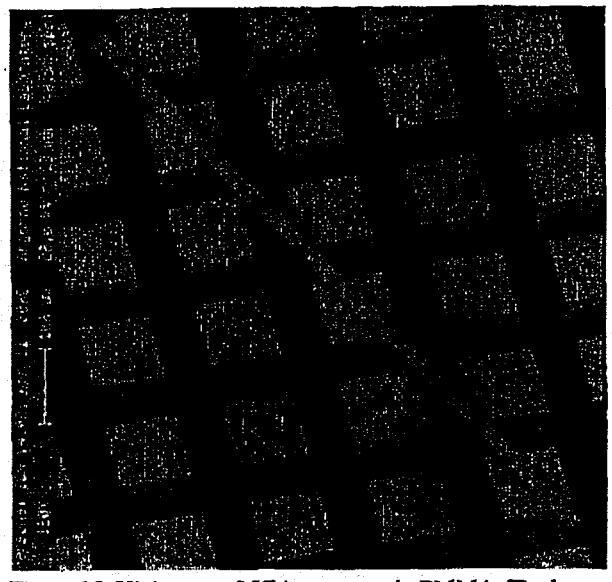

Figure 15: High aspect LIGA exposure in PMMA. The long narrow column has broken off from another area of the exposure.

6. Discussion

We have produced the first focusing result from a LIGA test sample. While the quality of the image is not particularly good, we are greatly encouraged as our measured roughness figures suggested that no focal image was likely. In order to improve LIGA samples to a point where they are comparable with MCPs, the surface roughness must be reduced by a factor of 5 at least. Methods of obtaining the surface improvement include annealing or an applied coating. We also believe that investigating different exposure energies and developing regimes will be fruitful. The taper angle must also be reduced in order to produce a high quality focus. We believe that pursuing different exposure energies and developing regimes may also be useful in reducing taper. There are reported examples of taper angle as low as 0.4 mrad[16]. Finally, our preliminary work with deep-etch LIGA suggests that pursuing 50:1 aspect ratios for our channels is possible.

ACKNOWLEDGMENTS

AGP acknowledges receipt of an ARC post-doctoral fellowship and of an ARC Small grant. THKI acknowledges receipt of an ARC postgraduate award.

REFERENCES

1. J. R. P. Angel, ApJ **233**, 364 (1979).
2. H. N. Chapman, K. A. Nugent, and S. W. Wilkins, Rev. Sci. Instrum. **62**, 1542 (1991).
3. A. G. Peele, K. A. Nugent, A. V. Rode, K. Gabel, M. C. Richardson, R. Strack, and W. Siegmund, Appl. Opt. **35**, 4420 (1996).
4. W. C. Priedhorsky, A. G. Peele, and K. A. Nugent, MNRAS **279**, 733 (1996).
5. M. W. Beijersbergen, M. Bavdaz, A. J. Peacock, E. Tomaselli, G. Fraser, A. Brunton, E. Flyckt, M. K. Krumrey, and A. Souvorov, Proc. SPIE **3765**, 452 (1999).
6. A. N. Brunton, A. P. Martin, G. W. Fraser, and W. B. Feller, Nucl. Instrum and Meth. A **431**, 356 (1999).
7. A. G. Peele, G. W. Fraser, A. N. Brunton, A. P. Martin, R. M. Rideout, N. E. White, R. Petre, and W. B. Feller Proc. SPIE **3444**, 404 (1998).
8. A. G. Peele, Rev. Sci. Instrum. **70**, 1268 (1999).
9. T. Irving, A. G. Peele, K. A. Nugent, and S. Brumby In preparation (2000).
10. 10500 S.W. Nimbus Avenue, Tigard, OR 97223-4310, USA
11. A. G. Peele, B. E. Allman, V. Cucevic, A. Cimmino, K. A. Nugent, S. W. Wilkins, H. N. Chapman, SPIE **2015**, 118 (1994).
12. R. Hudec, L. Pina, A. Inneman, P. Gorenstein, Astronomische Nachrichten **319**, 145 (1998).
13. H. N. Chapman, A. Rode, K. A. Nugent, S. W. Wilkins, Appl. Opt. **32**, 6333 (1993).
14. A. N. Brunton, G. W. Fraser, J. E. Lees, and I. C. E. Turcu, Appl. Opt. **36**, 5461 (1997).
15. P. Beckmann, A. Spizzichino, The Scattering of Electromagnetic Waves from Rough Surfaces, Pergamon Press, Oxford, 1963
16. C. R. Friedrich *et al*, in *Handbook of Microlithography, Micromachining, and Microfabrication Volume 2: Micromachining and Microfabrication*, 1st edition, edited by P. Rai-Choudhury (SPIE Optical Engineering Press, Bellingham, 1997), Vol. 2, Chap. 6, p.315.